Available online at www.sciencedirect.com

ScienceDirect

www.elsevier.com/locate/jes

JES JOURNAL OF ENVIRONMENTAL SCIENCES

www.jesc.ac.cn

A new method of simultaneous determination of atmospheric amines in gaseous and particulate phases by gas chromatography-mass spectrometry☆

Yifei Chen[1,2], *Qinhao Lin*[1,2], *Guiying Li*[1,2], *Taicheng An*[1,2,3,*]

[1] *Guangdong-Hong Kong-Macao Joint Laboratory for Contaminants Exposure and Health, Guangdong Key Laboratory of Environmental Catalysis and Health Risk Control, Institute of Environmental Health and Pollution control, Guangdong University of Technology, Guangzhou 510006, China*

[2] *Guangzhou Key Laboratory of Environmental Catalysis and Pollution Control, Key Laboratory of City Cluster Environmental Safety and Green Development (Department of Education), School of Environmental Science and Engineering, Guangdong University of Technology, Guangzhou 510006, China*

[3] *Chemistry and Chemical Engineering Guangdong Laboratory, Shantou 515031, China*

ARTICLE INFO

Article history:
Received 19 July 2021
Revised 16 September 2021
Accepted 22 September 2021
Available online 20 February 2022

Keywords:
Atmospheric amines
Determination method
Simultaneous determination
Gaseous and particulate phases
Gas chromatography-mass spectrometry

ABSTRACT

As more attention is being paid to the characteristics of atmospheric amines, there is also an increasing demand for reliable detection technologies. Herein, a method was developed for simultaneous detection of atmospheric amines in both gaseous and particulate phases using gas chromatography-mass spectrometry (GC-MS). The amine samples were collected with and without phosphoric acid filters, followed by derivatization with benzenesulfonyl chloride under alkaline condition prior to GC-MS analysis. Furthermore, the method was optimized and validated for determining 14 standard amines. The detection limits ranged from 0.0408-0.421 μg/mL (for gaseous samples) and 0.163-1.69 μg/mL (for particulate samples), respectively. The obtained recoveries ranged from 68.8%-180% and the relative standard deviation was less than 30%, indicating high precision and good reliability of the method. Seven amines were simultaneously detected in gaseous and particulate samples in an industrial park using the developed method successfully. Methylamine, dimethylamine and diethylamine together accounted for 76.7% and 75.6% of particulate and gaseous samples, respectively. By comparing the measured and predicted values of gas-particle partition fractions, it was found that absorption process of aqueous phase played a more important role in the gas-partition of amines than physical adsorption. Moreover, the reaction between unprotonated amines and acid (aq.) in water phase likely promoted water absorption. Higher measured partition fraction of dibutylamine was likely due to the reaction with gaseous HCl. The developed method would help provide a deeper understanding of gas-particle partitioning as well as atmospheric evolution of amines.

© 2022 The Research Center for Eco-Environmental Sciences, Chinese Academy of Sciences. Published by Elsevier B.V.

☆ This article is dedicated to Professor Dianxun Wang.

* Corresponding author.
E-mail: antc99@gdut.edu.cn (T. An).

https://doi.org/10.1016/j.jes.2021.09.027
1001-0742/© 2022 The Research Center for Eco-Environmental Sciences, Chinese Academy of Sciences. Published by Elsevier B.V.

Introduction

Amines are the one of the most important nitrogen-containing organics in atmosphere, which affect human health and actively participate in physical as well as atmospheric chemical reactions (Liu and Du, 2020), such as the formations of new particles and brown carbon (De Haan et al., 2011). Atmospheric amines have various natural and anthropogenic sources, such as evaporation from ocean, biomass burning, vegetation, and some geologic activities (Shen et al., 2017; Zhou et al., 2019). Most of the aromatic amines from anthropogenic sources are linked with fish processing, chemical industry and leather manufacturing (Ge et al., 2011a). Additionally, with increasing attention to climate change, amines are widely used as effective absorption solvents for capturing CO_2 for combustion process (Ge et al., 2014; Varghese and Karanikolos, 2020). Therefore, carbon sequestration is considered as another anthropogenic source of atmospheric amines (Nielsen et al., 2012). Gaseous amines, including methylamine (MA), dimethylamine (DMA) and trimethylamine (TMA), are highly hazardous and toxic, and usually have an unpleasant smell (Ge et al., 2011a; Li et al., 2019; Qiu et al., 2021). Although they are not very detrimental at typical ambient concentrations, the occurrence of amine conversion and degradation products which are also carcinogenic, or frequent exposure to these anthropogenic sources might elevate human health risk (Chhibber-Goel et al., 2016; Nielsen et al., 2012).

In addition, amines have been proved to promote the formation and growth of neutral and ionic clusters (Kürten et al., 2014; Zhang et al., 2021), even when their concentration is several orders of magnitude lower than that of NH_3. It has been reported that the particle formation rate of DMA was 1000 times higher than that of NH_3 when DMA level was higher than 3 pptv (Almeida et al., 2013). Partitioning of gaseous amines into particles and subsequent displacement of ammonium in the particles would also increase the concentration of amines on particles (Huang et al., 2014). This might further modify pH value and contribute to the brown carbon formation from the reaction of amines with carbonyl compounds (e.g., glyoxal) (De Haan et al., 2011). On the contrary, a study on ammonium formation from the reaction of gaseous amines with NO_x during photooxidation process showed that amines repartition from ammonium back to gaseous phase with the decrease in level of the parent amines in gaseous phase (Murphy et al., 2007). Therefore, simultaneous observation of amines in both gaseous and particulate phases would provide a deeper understanding of the evolution of amines in atmosphere.

Measurement of gaseous amines is typically performed using online techniques including ambient pressure proton transfer mass spectrometry (AmPMS) (Hanson et al., 2011), high-resolution time-of-flight chemical ionization mass spectrometer (HR-ToF-CIMS) (You et al., 2014), and chemical ionization atmospheric pressure interface time-of-flight mass spectrometry (CI-APi-TOF-MS) (Simon et al., 2016). Other online techniques, such as aerosol time-of-flight mass spectrometry (ATOFMS) (Healy et al., 2015), single-particle aerosol mass spectrometry (SPAMS) (Chen et al., 2019), atmospheric pressure interface time-of-flight mass spectrometry (APi-TOF-MS) (Junninen et al., 2010) and thermal desorption chemical ionization mass spectrometry (TDCIMS) (Smith et al., 2010), have also been used to detect amines deposited onto particles. Although these online techniques are attractive in their ability to analyze the evolution of atmospheric amines with a high time resolution (Healy et al., 2015; You et al., 2014), the simultaneous determination of amine species in both gaseous and particulate phases has not been attempted yet.

Compared with online instruments, off-line methods can provide greater selectivity or better separation for amine monitoring (Jastrzebska et al., 2014). Many off-line methods have also been developed for amine determination in gaseous or particulate phases due to their simplicity, high resolving power and sensitivity, especially in the analysis of very complex mixtures. Gas chromatography (GC) coupled with mass spectrometry (GC-MS) method has been widely used for detecting atmospheric amines. However, there are very few methods for simultaneous determination of amines in both gaseous and particulate phases. Most of the methods only focus on the particulate phase or gaseous phase. Akyüz (2007) reported the simultaneous determination of thirty-four amines in $PM_{2.5}$, PM_{10} and gaseous phase using isobutyl chloroformate as the derivatization reagent. In their work, 0.1 mol/L HCl solution was used to absorb gaseous phase amines, but the collection and derivatization processes are complex and the liquid absorption equipment is not easy to handle or transport. A faster and simpler derivatization method was developed using benzenesulfonyl chloride (BSC) as the derivatization reagent to elucidate the characteristics of amines in particulate phase (Liu et al., 2017). However, the conditions of derivatization have not been discussed in detail.

The aim of this study was to develop a new method for simultaneous determination of atmospheric amines in both gaseous and particulate phases with BSC derivatization by GC-MS, coupled with a commonly used method to collect gaseous and particulate amines using phosphoric acidified filter (Kieloaho et al., 2013; Rampfl et al., 2008). An in-depth evaluation of this new developed method was performed to optimize the influence of amount of BSC and alkali condition on the derivatization procedure. Furthermore, the developed method was successfully validated in simultaneous measurement of the concentration of gaseous and particulate amines in an industrial district in China.

1. Materials and methods

1.1. *Reagents and instruments*

The details of the reagents and instruments used in this work are provided in Appendix A. Supplementary data. The structures and molecular weights of the 14 tested amines are all shown in **Table S1**. The 14 amines are methylamine (MA), dimethylamine (DMA), ethylamine (EA), propylamine (PA), diethylamine (DEA), butylamine (BA), *tert*-butylamine (TBA), cyclohexylamine (CA), dipropylamine (DPA), hexylamine (HA), benzylamine (BMA), dibutylamine (DBA), di-*n*-amylamine (DAA), and dihexylamine (DHA). GC-MS (Agilent 7890B-5977B, USA) was used to analyze the amines.

1.2. *Sampling site and sampling procedure*

Six parallel samples of particulate and gaseous phases were collected from Guangzhou Industrial Park between 17 to 19 June, 2020, and each sample was collected for 8 hr continuously. Environmental variables (e.g., temperature and relative humidity (RH, %)) were routinely monitored during this period. The sampling site is located in an open square in the Industrial Park with logistics, chemical and pharmaceutical industries. Two layers of quartz filters were placed in a total suspended particulate (TSP) high flow sampler (Tianhong Instruments Inc., flow rate of 0.65 m^3/min). The upper filter was used to collect amines in particulate phase and the lower filter (soaked with 5 vol.% (by volume) methanol phosphate (referred to as acid filter below)) was used to collect gaseous amines. The filters were initially baked for 4 hr in a muffle furnace at 500°C. Before weighing, all filters were kept in a chamber (at 20°C, relative humidity of 30%) for 24 hr, and then transported to the laboratory and stored at -20°C until sampling.

Sampling artifact analysis included the collection efficiency of acidified membrane and the influence of particles in the first layer. Three layers of filters were placed in the same sampler for sampling to evaluate the absorption rate. The first layer was a blank phosphate free filter, and the second and third layers were the same batch of phosphate containing filters. Two samplers were used for parallel sampling to evaluate the influence of particles in the first layer. The second layer of filter of both samplers was phosphate acidified filter. The first layer in one sampler was blank (defined as the control group), and the first layer of the other sampler was a filter containing a certain amount of particles (defined as the experimental group). The samples involved in sampling artifact analysis were collected on the roof of the teaching building of the School of Environment, Guangdong University of Technology. Each sample was collected for 8 hr continuously, with the flow rate of 0.65 m^3/min and the relative humidity of 73%.

1.3. *Derivatization procedures*

Mixed standard solution was dissolved in methanol to reach a concentration of 100 μg/mL for each standard amine. NaOH solution (200 μL 10 mol/L) and BSC (200 μL) were added into a brown vial with non-acidified filter extract, and 1000 μL NaOH solution (10 mol/L) and 200 μL BSC were added into another brown vial with acidified filter extract. The vials were closed and agitated using a magnetic stirrer at room temperature for 30 min. Another 0.5 mL of NaOH solution (10 mol/L) was added into the vials and agitated at 80°C for another 30 min. The mixed solution was cooled down to room temperature and transferred into a Teflon centrifuge tube, and then the pH was adjusted to 5.5 with 36.5 wt.% HCl solution. The mixed solution was extracted with 3 mL dichloromethane for three times, and mixed with a shaking mixer for 1 min each time. The organic phase was washed with 3 mL Na_2CO_3 solution (0.05 mol/L) and then dried with anhydrous sodium sulfate. The internal standard indicator hexamethylbenzene was added and the volume was fixed to a specific volume for later analysis.

Part of each sample was ultrasonically extracted with ultrapure water for 15 min, and the process was repeated three times. A total of 20 mL extracted solution was transferred into a flat bottom flask. The derivatization of amines in extracted solution was performed using the above processes. Note that the volume of BSC was optimized as 200 μL for derivatization of all amines in extracted solution, and 200 and 1000 μL 10 mol/L NaOH solution for particulate and gaseous amines, respectively, as discussed in Section 2.2. All samples were spiked with DMA-d6 as the recovery standard.

1.4. *GC-MS analysis*

All amines were analyzed using GC-MS. The chromatographic column employed was a 30 m HP-5MS column (i.d. 0.25 mm, 0.25 μm film thickness, 19091S-433UI, Agilent, USA). The GC temperature program was as follows: initial temperature was 80°C, held for 1 min, and then continuously programmed heating to 180°C at 5°C/min, then to 240°C at 10°C/min, 290°C at 25°C/min and finally held for 10 min. The injector and transfer line temperatures were both maintained at 290°C. Helium was used as a carrier gas and the flow rate was set as 1 mL/min. Splitless injection mode of a 1 μL sample was performed. Electron energy was set at 70 eV and the mass scan range of mass-to-charge ratio (*m*/*z*) 50-450 was monitored.

Then, 20 μL of 100 μg/mL mixed standard solution of amines was added and then followed by the above derivatization processes. Furthermore, each amine was diluted to varied concentrations (i.e., 0.5, 1.0, 2.0, 5.0, 8.0, 10.0, 15.0, 20.0, 25.0 μg/mL) for the establishment of calibration curve. The limit of detection (LOD) and limit of quantification (LOQ) of each amine are defined as three and ten times of the signal-to-noise ratio (*S*/*N*), respectively. Three spiking amounts of 500, 1000 and 5000 ng for each amine were selected to determine the recoveries (characterization of loss during membrane extraction) and relative standard deviation (RSD).

1.5. *Statistical methods*

SPSS V26.0 was used to compare the effects of variables, and the data were analyzed using Analysis of Variance (ANOVA) statistical tests (including one-way analysis and Welche's analysis), and multiple comparison (including post-hoc Tukey tests and Games-Howell test). The analysis process is shown in **Fig. S1**. Variables of interest for these tests included amount of BSC and NaOH for particulate and gaseous amine detection, respectively. Normality test was used to determine whether the data were suitable for ANOVA statistical tests, and the results were expressed by significance (Sig.), as shown in **Table S2**. The significance results of the test data were higher than 0.05, suggesting that ANOVA analysis was suitable for the data in this study. ANOVA results (*p*-value) higher than 0.05 indicate that the variable has no impact on derivatization efficiency of amines, while *p*-value less than 0.05 indicates that it has an obvious influence. Then, multiple comparison was used to identify the subset with the best average efficiency under different dosages. The efficiency of each dosage in this subset was equivalent. The details of calculations and statistical process are provided in Appendix A. Supplementary data.

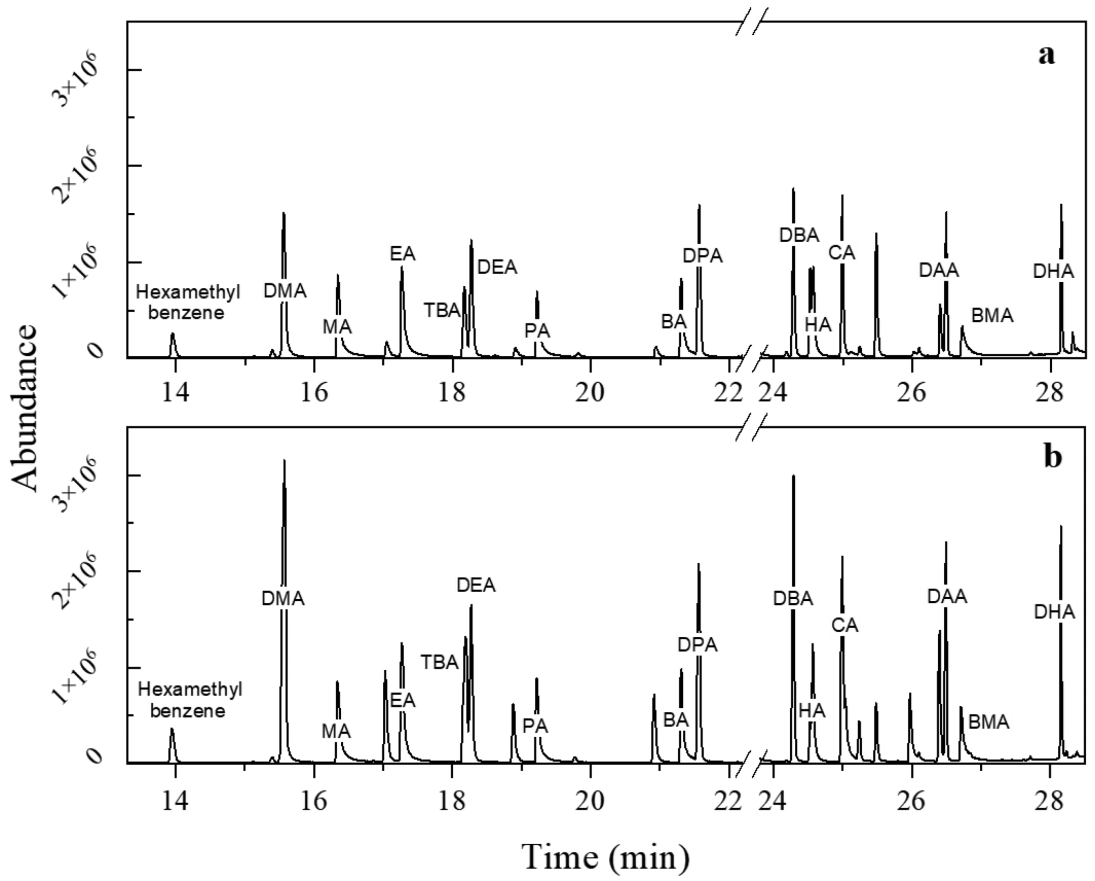

Fig. 1 – Total ion chromatography of 14 amines derived in (a) non-acid filter extract and (b) acid filter extract.

2. Results and discussion

2.1. *Analytical method*

Currently, various derivatizing reagents are used to prevent interaction of the strong dipole between amines and silanol groups or siloxane bridges, to allow the measurement of amines using GC-MS (Fekete et al., 2010). BSC is frequently selected as derivatization reagent because it can react with amines to form derivatives with low polarity. Previously, BSC was used as a derivatization reagent to determine the concentration of 17 amines in river (Zhang et al., 2012) and 9 amines in $PM_{2.5}$ (Liu et al., 2017). A total of 14 standard amines were measured using the BSC derivatization method in this study. Among the tested amines, the analysis of TBA, DHA, DAA and CA has not been reported in previous studies. **Fig. 1** shows the total ion chromatography of 14 standard amines. Their retention time, qualitative ions and quantitative ions are listed in **Table 1**. The retention times of 14 standard amines ranged from 15.73 to 28.24 min, which was more time saving than the method developed by Akyüz (Akyüz, 2007), whose time spent was about 60 mins. Moreover, some isomers, such as TBA, BA and DEA, HA and DPA, could be well separated (**Fig. 1a**). For instance, there were no tailing peaks in the chromatogram between TBA and DEA which can be easily distinguished, despite the similar retention times of TBA (18.34 min) and DEA (18.44 min).

According to the reaction formula of organic amines and BSC, HCl is formed after reaction. Then, the addition of alkali consumes the generated HCl and makes the reaction move forward. **Fig. S2** shows derivatization efficiencies of 14 standard amines in the absence and presence of NaOH. It was found that the derivatization efficiencies of 14 amines increased by 5%-70% in the presence of NaOH relative to the absence of NaOH. This indicates that the presence of NaOH solution improves derivatization efficiency of amines and alkaline conditions are necessary for the derivatization of BSC. In this study, a quartz filter acidified by phosphoric acid and a non-acidified filter were placed in a sampler to simultaneously collect gaseous and particulate amines. To completely collect gaseous amines, excess phosphoric acid was used in the filter, so that its extract was acidic. Therefore, more alkali was added in the treatment of gaseous samples than particulate samples. **Fig. 1b** shows the total ion chromatography results of 14 amines derived by BSC in the extract of acidified filters, indicating that the derivatization method of BSC can be used for the pretreatment of gaseous amines.

2.2. *Optimization of derivatization*

For unknown samples, excess derivatization reagents are usually added to ensure that various amines be fully derivatized (Huang et al., 2014). However, an optimum volume of derivatization reagent has not been described in the previous stud-

Table 1 – Retention time, qualitative ions and quantitative ions of atmospheric amines.

No.	Compounds	Retention time (min)	Qualitative ion and quantitative ion (*m*/z)
1	Methylamine (MA)	16.50	77, 106, 141, **171**
2	Dimethylamine (DMA)	15.73	77, 120, 141, **185**
3	Ethylamine (EA)	17.43	77, 141, 170, **185**
4	Diethylamine (DEA)	18.44	77, 141, **198**, 213
5	Propylamine (PA)	19.38	77, 78, 141, **170**,199
6	Dipropylamine (DPA)	21.72	77, 141, **170**, 212
7	*tert*-Butylamine (TBA)	18.34	77, 141, **198**
8	Butylamine (BA)	21.46	77, 141, 158, **170**, 213
9	Dibutylamine (DBA)	24.41	77, 141, 170, 184, **226**
10	Cyclohexylamine (CA)	25.11	77, 98, **196,** 239
11	Hexylamine (HA)	24.69	77, 100, 141, 158, **170**, 241
12	Di-*n*-amylamine (DAA)	26.61	77, 140, 98, **184,** 240
13	Benzylamine (BMA)	26.82	77, **106**, 125, 143
14	Dihexylamine (DHA)	28.24	77, 141, **184,** 254
15	Aniline (AE)	25.37	77, 141, **210**, 253

Bold words represent the quantitative ion.

ies (Liu et al., 2017; Zhang et al., 2012). To determine the optimum volume of BSC, in this study, a series of BSC volumes were set up ranging from 25 to 400 μL, corresponding to molar ratios of BSC to total amine ($BSC/amines_{total}$) ranging from 149 to 2363. Derivatization efficiencies of various amines with different BSC volumes were expressed by peak areas of their derivatization products. Furthermore, the data were analyzed using ANOVA statistical tests to evaluate whether BSC volume affects the derivatization efficiency. As seen from **Table S3**, except for BMA (p-value = 0.176), the p-values of other amines were less than 0.05, indicating that the amount of BSC had a great influence on their derivatization efficiencies. To further obtain the optimal amount of BSC, a multiple comparison was also performed (**Tables S4** and **S5**). Take DHA for example, the parallel data of DHA at one BSC dosage were classified into a group, and the groups with different BSC dosages were divided into three subsets by multiple comparison (**Table S4**). The third subset with the largest serial number corresponded to the subset with the best average derivatization efficiency. Based on the principle of green chemistry, in the third subset, the minimum amount (25 μL) was the best derivative volume for DHA. Similarly, 25 μL of BSC was the optimized volume to achieve the highest derivatization efficiency for BMA and DHA (**Fig. S3a**), 50 μL for PA, DPA, CA, HA, DAA, BA, and DBA (**Fig. S3b**), and 100 μL for MA, DMA, and DEA (**Fig. S3c**). It should be pointed out that, for EA and TBA, reasonable results could not be obtained using only the method based on homogeneous subsets. Hence, Games-Howell multiple comparison was used to modify the results of homogeneous subsets (**Table S5**). It was found that 100 μL BSC was the optimized choice for EA, and 200 μL for TBA (**Fig. S3d**). Therefore, 200 μL BSC (when $BSC/amines_{total}$ >1182, i.e. total mass of amines was 56 μg) was selected as the optimized volume to ensure sufficient derivatization efficiency of each amine in this study.

As discussed in Section 2.1, NaOH played an important role in increasing the derivatization efficiency of BSC. However, it is still not clear whether more amount of NaOH can lead to better derivatization efficiency. Therefore, to obtain the optimal volume, different volumes of NaOH (10 mol/L) including 200, 400, 600, 800 and 1000 μL were used for estimating derivatization efficiency of amines. As **Fig. S4** shows, the derivatization efficiency of 14 amines did not increase with increase in NaOH volume. According to the one-way ANOVA analysis, the p-values of amines ranged from 0.074-0.861 and were higher than 0.05, except for MA ($p = 0.015$), EA ($p = 0.041$ and DEA ($p = 0.015$) (**Table S6**). These results indicated that increase in volume of NaOH cannot enhance the derivatization efficiency of amines. The results of MA, EA and DEA using the multiple comparison method showed that the optimal volume of NaOH was 200 μL (**Table S7**). This value was consistent with the results of the other 11 amines. Thus, 200 μL of 10 mol/L NaOH solution was the optimal volume for the BSC derivatization of amines.

In this study, a quartz filter acidified by phosphoric acid and a non-acidified filter were placed in a sampler to simultaneously collect gaseous and particulate amines, respectively. Amines collected in the phosphoric acid and non-acidified filters were extracted with ultrapure water to further measure their species and concentration using the BSC derivatization method. To completely absorb gaseous amines, excess phosphoric acid was used in the filter, resulting in an acidic environment. Therefore, more alkali should be added in the treatment of gaseous samples than particulate samples, because the gaseous samples include a large amount of phosphoric acid.

Herein, different volumes (800, 1000, 1200, 1400 and 1600 μL) of NaOH solution (10 mol/L) were used to determine the optimal alkali volume for measurement of gaseous amines. As **Fig. S5** shows, except for TBA and MA, the derivatization efficiency of other amines increased by 3%-50% with increase in volume of NaOH from 800 to 1000 μL. However, there were obvious changes in the derivatization efficiency of 14 amines

Table 2 – limit of detection (LOD), limit of quantification (LOQ) and parameters of the calibration curves for atmospheric amines in gaseous and particulate.

No.	Compounds	Linear range (μg/mL)		Correlation coefficient (R^2)		LOD (μg/mL)	LOQ (μg/mL)
		Gaseous amines	Particulate amines	Gaseous amines	Particulate amines		
1	DMA	0.5-25.0	0.5-25.0	0.995	0.998	0.0845	0.338
2	MA	1.0-25.0	1.0-25.0	0.996	0.998	0.421	1.686
3	EA	1.0-25.0	1.0-25.0	0.992	0.997	0.121	0.484
4	DEA	0.5-25.0	0.5-25.0	0.997	0.998	0.421	0.432
5	TBA	1.0-25.0	1.0-25.0	0.992	0.995	0.0818	0.327
6	PA	0.5-25.0	0.5-25.0	0.993	0.999	0.126	0.502
7	DPA	0.5-25.0	0.5-25.0	0.995	0.998	0.114	0.454
8	BA	0.5-25.0	0.5-25.0	0.993	0.997	0.156	0.624
9	DBA	0.5-25.0	0.5-25.0	0.998	0.997	0.0993	0.397
10	CA	0.5-25.0	0.5-25.0	0.996	0.993	0.0818	0.327
11	HA	0.5-25.0	0.5-25.0	0.996	0.998	0.145	0.579
12	BMA	1.0-25.0	1.0-25.0	0.996	0.996	0.0408	0.163
13	DAA	0.5-25.0	0.5-25.0	0.997	0.997	0.178	0.712
14	DHA	0.5-25.0	0.5-25.0	0.994	0.997	0.125	0.499

with NaOH volumes above 1000 μL. Based on the one-way ANOVA analysis, as the NaOH volumes increased from 1000 to 1600 μL, the *p*-values of 14 amines ranged from 0.051-0.909 (**Table S8**), all of which were higher than 0.05. This further confirmed that NaOH volume above 1000 μL had a minor effect on derivatization efficiency of amines. Therefore, for the detection of gaseous amines, 1000 μL of 10 mol/L NaOH solution was the optimal amount. The overall optimal conditions for simultaneous detection of amines in gaseous and particulate phases were 200 μL BSC for both gaseous and particulate samples, as well as 200 and 1000 μL 10 mol/L NaOH solution for particulate and gaseous samples, respectively.

2.3. *Method validation*

The collection efficiency (η) in this study was calculated by Eq. (1):

$$\eta = \frac{c_{second}}{c_{second} + c_{third}} \times 100\% \quad (1)$$

where c_{second} and c_{third} (ng/m^3) are the concentrations of amines in second and third layers, respectively. As seen from the results in **Table S9**, the collection efficiency of total amines detected was 95.8% ± 0.48%, indicating that second layer filter was enough for collection.

The influence of particles in the first layer is expressed by ratio α in this study, which can be calculated by Eq. (2):

$$\alpha = \frac{|c_{exp} - c_{con}|}{c_{exp}} \times 100\% \quad (2)$$

where c_{con} and c_{exp} (ng/m^3) are the concentrations of total gaseous amines in control and experimental groups, respectively. As shown in **Table S9**, the α value of total amines detected was 1.7% ± 0.95%, indicating that the contribution of gaseous amines related to particles in the first layer accounted for a small part. Therefore, the influence of particles in the first layer can be ignored.

Table 2 summarizes the parameters of the calibration curves for particulate and gaseous amines, including linear range, correlation coefficient (R^2), LOD and LOQ. Calibration curves of particle amines detection method (hereafter referred to as particle method) and gaseous amines detection method (hereafter referred to as gaseous method) were developed for amine concentrations varying from 0.5 to 25 μg/mL, and the quantification was performed using the internal standard method. High R^2 values in the range of 0.992-0.998 and 0.993-0.999 were observed for the calibration curves of 14 amines for particle and gaseous methods, respectively. The calculated LOD and LOQ obtained from GC-MS results based on "$S/N = 3$" and "$S/N = 10$" were within the range of 0.0408-0.421 and 0.163-1.68 μg/mL, respectively.

Three spiking amounts of 500, 1000 and 5000 ng for each amine were selected to determine the recoveries (characterization of loss in membrane extraction) and RSD. The RSD refers to the ratio of standard deviation to arithmetic mean of measured results, which reflects the precision and reproducibility of the obtained results. The recoveries and RSDs of 14 amines with particle and gaseous methods are listed in **Table S10**. The recoveries of all amines using particle and gaseous methods were 65.8%-133% and 68.0%-180%, respectively. The RSD for particle and gaseous methods were both less than 30%. Therefore, the method established in this study can be used to quantify amines in gaseous and particulate samples.

2.4. *Environmental application*

To verify the feasibility of this developed method in environmental application and explore the transformation of gaseous amines into particles, six parallel samples of particulate and gaseous phases were collected in the Guangzhou industrial park for three days. The average relative humidity during sampling was 81% and the temperature was 33°C. The detailed weather parameters of the industrial park can be found in **Table S11**.

Seven amines including MA, DMA, EA, DEA, CA, DBA and TBA were found in gaseous and particulate phases. Their total concentration in gaseous phase was 238 ng/m^3, which was

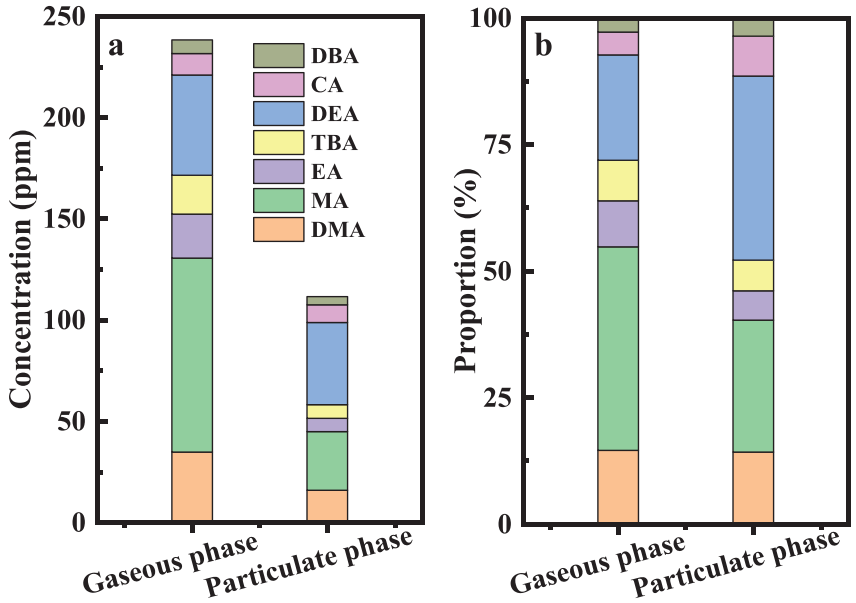

Fig. 2 – (a) Concentration and (b) relative abundance of atmospheric amines in gaseous, TSP samples.

more than two times higher than that in particulate phase (**Fig. 2**). In gaseous phase, MA, DMA and DEA were the main organic amines, and their concentrations were 95.9 ± 44.1, 34.8 ± 31.7, and 49.5 ± 38.6 ng/m^3, which accounted for 40.2%, 14.6%, and 20.8% of total seven amines, respectively. In particulate phase, MA, DMA and DEA were also the main amines, and their concentrations were 29.1 ± 25.8, 16.0 ± 7.39, and 40.6 ± 19.0 ng/m^3, accounting for 26.1%, 14.3%, and 36.4% of total seven amines, respectively.

A previous study of urban district in Guangzhou found that the main amines in $PM_{2.5}$ are MA, DMA and DBA, while DEA accounts for a small proportion (Cheng et al., 2019; Liu et al., 2017). In contrast, DEA accounted for a large proportion (up to 36%) of particulate samples in the industrial park in this work. In addition, previous studies (Ho et al., 2016; Perrone et al., 2016) only found low weight amines with simple structure. However, in this study, small proportions of CA (4% and 8%) and TBA (8% and 6%) with higher weight or complex structure were also found in both gaseous and particulate phases, which may come from the chemical sources (Ge et al., 2011a).

Furthermore, two different processes were used to describe the gas-particle partitioning of amines, namely, physical adsorption onto aerosol surface and absorption into condensed phase (Ge et al., 2011b; Lohmann and Lammel, 2004). The measured fraction of gas-particle partition of amines (Φ(Meas.)) can be described by Eq. (3) (Lohmann and Lammel, 2004),

$$\Phi(\text{Meas .}) = \frac{c_p}{c_p + c_g} \times 100\% \quad (3)$$

where, c_p and c_g (ng/m^3) are the concentrations of particulate and gaseous phase amines, respectively. The measured fractions of gas-particle partition (Φ(Meas.)) of seven amines in this study were as follows: DMA 38% ± 25%, MA 24% ± 21%, EA 23% ± 2%, TBA 33% ± 37%, DEA 49% ± 29%, DBA 37% ± 6% and CA 43% ± 16% (**Fig. 3**). The Φ(Meas.) values of DMA and MA in this study were higher than those reported by Liu et al. (DMA 3.6%, and MA 14% in $PM_{2.5}$) (Liu et al., 2018).

The fraction of gas-particle partition through physical adsorption can be predicted by Junge-Pankow adsorption (J-P model, p_L^o-based) (Bidleman, 1988),

$$\Phi_{\text{adsorption}}(\text{Pred .}) = \frac{c\theta}{p_L^o + c\theta} \times 100\% \quad (4)$$

where, c is a constant (typically 17.2 Pa•cm) which relates to the heat of condensation of the chemical and the surface properties. The particle surface area per unit volume of air, θ, is often assumed to be 1.1 × 10^{-5} cm^2/cm^3 for urban air (Bidleman, 1988). p_L^o (atm) is the subcooled liquid vapor pressure of amine (the value of each amine can be found in **Table S12**). The predictive fractions of physical adsorption process ($\Phi_{\text{adsorption}}$(Pred.)) for seven amines in this study ranged from (4.7 × 10^{-5})% - (5.6 × 10^{-8})% (**Fig. 3**), which were 5-8 orders of magnitude lower than the measured value. This is different from polybrominated diphenyl ethers, which are neutral semi volatile organic compounds and their simulated adsorption values are similar to the measured values (An et al., 2011).

In the atmosphere, as a kind of free base with strong polarity, amines dissolve directly in the condensed liquid phase (including water phase, high polarity organic phase and low polarity organic phase) (Eq. (5)), and then react with H^+ to form salt in water phase (Eq. (6)). Moreover, they also dissolve in the liquid phase through acid-base reaction (Eq. (7)) (Ge et al., 2011b; Nielsen et al., 2012; Qiu and Zhang, 2013).

$$Am_{(g)} \rightleftharpoons Am_{(aq)} \quad (5)$$

$$Am_{(aq)} + H^+ \rightleftharpoons AmH^+_{(aq)} \quad (6)$$

$$Am_{(g)} + HX_{(g)} \rightleftharpoons AmX_{(s)} \quad (7)$$

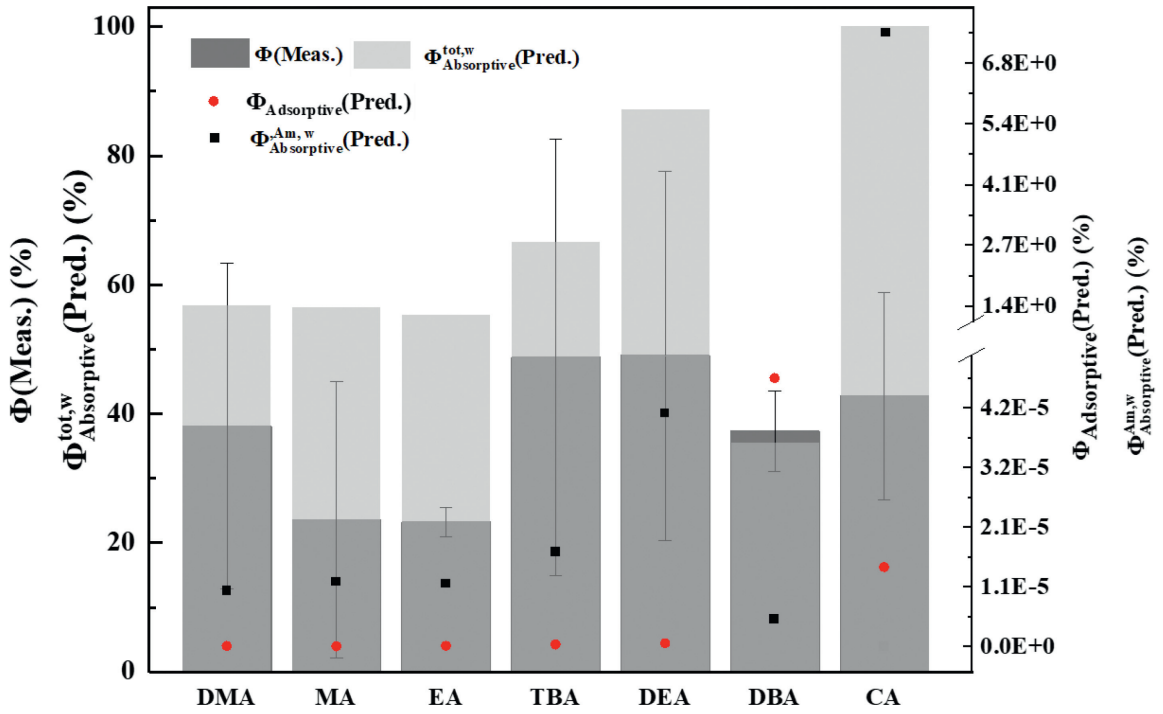

Fig. 3 – Comparing with the measured fraction (Φ(Meas.)) of seven amines in particle and their theoretical predictive fraction through physical adsorption ($\Phi_{adsorption}$(Pred.)) and absorption without acid-base reaction in aqueous phase ($\Phi^{Am,\ w}_{absorption}$(Pred.)) and with acid-base reaction ($\Phi^{tot,\ w}_{absorption}$(Pred.)).

where Am represents neutral "free-base" and unprotonated monoamines, and $X^- = Cl^-$ or NO_3^-.

According to literature (Lohmann and Lammel, 2004), for the direct dissolution process in pure water Eq. (5), the fraction ($\Phi^{w}_{absorption,\ Am}$(Pred.)) of amines can be described as follows:

$$\Phi^{Am,\ w}_{absorption}(\text{Pred.}) = \frac{K^{w}_{p,Am}\ TSP}{K^{w}_{p,Am}\ TSP + 1} \times 100\% \quad (8)$$

where TSP (μg/m^3) is the concentration of total suspended particulate matter according to the filters. $K^{w}_{p,Am}$ is the constant for partitioning of unprotonated amines in water phase, and can be calculated by Eq. (9) (Pankow, 2015),

$$K^{w}_{p,Am} = \frac{\frac{K^{w}_{H}}{\gamma^{w}_{Am}} RT}{10^9} \quad (9)$$

where K^{w}_{H} (mol/(kg•atm)) is the Henry's gas law constant for partitioning to an aqueous phase, referenced to infinite dilution in water (which can be found in **Table S11**). γ^{w}_{Am} is the molal scale activity coefficient (dimensionless) of an amine in water phase, and that in dilute water is γ^{w}_{Am}=1. In this study, the predicted values of partition fraction for each amine ($\Phi^{Am,\ w}_{absorption}$(Pred.)) were as follows: DMA (9.8 × 10^{-6})%, MA (1.1 × 10^{-5})%, EA (1.1 × 10^{-5})%, TBA (1.7 × 10^{-5})%, DEA (4.1 × 10^{-5})%, DBA (4.8 × 10^{-5})% and CA 7.4% (**Fig. 3**). Amounts of seven amines, the $\Phi^{Am,\ w}_{absorption}$(Pred.) values of MA, DMA, EA, DEA, DBA, and TBA are 5-6 orders of magnitude lower than Φ(Meas.) value, and the $\Phi^{Am,\ w}_{absorption}$(Pred.) value of CA is significantly higher than others. These results indicate that it is easier to enter the water phase through direct dissolution process with unprotonated form in water phase.

In an aqueous solution which is at equilibrium with the gaseous phase, the total molality of amines is equal to the sum of the undissociated amine and the amine cation Pankow, 2015) (due to process of Eq. (6)). Thus, the fractions ($\Phi^{tot,\ w}_{absorption}$(Pred.)) of amines can be predicted by the following Eqs. (10) - (12) (Ge et al., 2011b),

$$\Phi^{tot,w}_{absorption}(\text{Pred.}) = 1/\left(1+\left(\frac{273.15}{T}\right) \times\left(\frac{1}{0.022414}\right)/\left(g_w/1000\times {}^{tot}K_H\right)\right) \times 100\% \quad (10)$$

$$\log_{10}{}^{tot}K_H \approx \log_{10}\left(\frac{K^{w}_{H}}{K_a}\right) - \text{pH} \quad (11)$$

$$\text{pH} = -\log_{10}\left(\gamma \times \frac{[H^+]_{ins}}{V}\right) \quad (12)$$

where, T (K) is the environmental temperature during sampling (here, T = 306.15 K) and (g_w (g/m^3)) refers to the amount of liquid water in the aqueous aerosol phase per m^3 of atmosphere. Aerosol solution volume (V (cm^3)), in situ acidity ($[H^+]_{ins}$ (nmol/m^3)) and activity coefficient (γ) were obtained by the model E-AIM (model AIM-I) (http://www.aim.env.uea.ac.uk/aim/aim.php) (Carslaw et al., 1995). According to the model, the average pH of condensed phase was 2.2 ± 0.13, and average g_w was 6.09 ± 2.30 μg/m^3 (parameters in Eq. (11) are listed in **Table 3**). ${}^{tot}K_H$ is the total Henry's Law constant of amines. When pH of aerosol is < 7, it can be calculated by Eq. (11) (Ge et al., 2011b), and the results are shown in **Table S12**. K_a represents the acidity constant on molal scale referenced to infinite dilution in water (the values are provided

Table 3 – Concentration of atmospheric seven amines in gaseous and particle samples, and the concentration of total suspended particles (TSP), inorganic cation and anion in particle.

Composition	Concentration	
	Gaseous	Particle
DMA (ng/m^3)	34.8 ± 31.7	15.6 ± 7.39
MA (ng/m^3)	95.9 ± 44.1	29.1 ± 25.8
EA (ng/m^3)	21.7 ± 10.7	6.45 ± 2.65
TBA (ng/m^3)	19.1 ± 22.6	6.76 ± 7.44
DEA (ng/m^3)	49.5 ± 38.6	40.6 ± 19.0
CA (ng/m^3)	10.7 ± 6.19	8.78 ± 7.90
DBA (ng/m^3)	6.66 ± 0.85	3.96 ± 0.63
Na^+ (μg/m^3)	-	12.6 ± 0.95
K^+ (μg/m^3)	-	3.24 ± 0.59
Mg^{2+} (μg/m^3)	-	1.99 ± 0.06
Ca^{2+} (μg/m^3)	-	17.1 ± 10.2
Cl^- (μg/m^3)	-	8.23 ± 4.89
NO_3^- (μg/m^3)	-	11.1 ± 9.39
Br^- (μg/m^3)	-	0.33 ± 0.13
SO_4^{2-} (μg/m^3)	-	1.35 ± 6.94
TSP (μg/m^3)		126 ± 21.6
pH	-	2.2 ± 0.13
In situ acidity ($[H^+]_{ins}$ (nmol/m^3))	-	132 ± 63.0
Activity coefficient (γ)	-	1.59 ± 0.28
Aerosol solution volume ($V_{aerosol}$ (10^{-4} cm^3))	-	1.52 ± 0.35
H_2O (μg/m^3)	-	6.09 ± 2.30

in **Table S12**). The $\Phi^{tot,\ w}_{absorption}$(Pred.) values of seven amines ranged from 35%-100%. The maximum of $\Phi^{tot,\ w}_{absorption}$(Pred.) was the value of CA (100%), and second one was DEA (87%), followed by DMA (57%), MA (56%) and, EA (55%) and the minimum was DBA (35%) (**Fig. 3**). This is consistent with the measured values of CA and DEA in this study, indicating that they are likely to enter the aqueous phase by direct dissolution. However, the lowest $\Phi^{tot,\ w}_{absorption}$(Pred.) of DBA suggested that its trend of direct dissolution in water phase was weak, and there may be other processes involved.

The predicted values of gas-particle partition fraction through three processes (including physical adsorption, simple gas-liquid conversion process (Eq. (5)), and gas-liquid conversion process considering protonation (Eq. (6)) were compared with the measured values (**Fig. 3**). The predicted values of physical adsorption and simple gas-liquid conversion in water phase were far less than the actual measured values (5-8 orders of magnitude difference), while the order of magnitude of the predicted value was the same as that of the measured. These results indicate that the absorption process of aqueous phase plays an important role in the gas-partition of amines, and the reaction between unprotonated amines and $acid_{(aq)}$ in water phase may promote water absorption. In addition, the measured value was lower than the $\Phi^{tot,\ w}_{absorption}$(Pred.) in this study, which may be due to some additional transformation pathways of amines, such as carbonyl-amine reactions (Qiu and Zhang, 2013) and oxidation reaction with O_3 or $^{\bullet}OH$ (Tong et al., 2020).

At present, there is no established simulation model to predict the gas-particle partition fraction based on the reaction between gaseous amines and gaseous acid (Eq. (7)). However, the K_p^*, dissociation constant of solid aminium nitrate or chloride (to form gaseous phase amine and HNO_3 or HCl) can be used to evaluate the partition law based on Eq. (7). At temperature above 298.15 K, the smaller the K_p^* value of amines, the greater the possibility of forming corresponding aminium salt (Ge et al., 2011b). Ge et al. (2011b) estimated that the possibility of salt formation of amines is as follows: for aminium chloride, DBA > DEA > MA >EA >DMA; for aminium nitrate, DEA > EA >DMA > MA. Moreover, a considerable number of [Cl^-] (8.23 ± 4.89 μg/m^3), as a second inorganic anion in the particle, can be found in this study. Thus, higher measured value (Φ(Meas.)) of DBA in this study is likely due to the reaction with gaseous HCl.

3. Conclusions

In this study, a new method was developed for simultaneous determination of gaseous and particulate amines using BSC derivatization. The optimal reaction conditions were 200 μL BSC (for all samples), as well as 200 μL (for particulate samples) and 1000 μL (for gaseous samples) NaOH (10 mol/L). The detection limits obtained by using GC-MS results based on "$S/N = 3$" and "$S/N = 10$" were within the range of 0.0408-0.4214 μg/mL (for gaseous samples) and 0.1630-1.6857 μg/mL (for particulate samples), respectively. The obtained recoveries ranged from 68.81% to 180.65% and the standard deviation of this method was < 30%, which indicates high precision and good reliability of the method. This method was further validated for the simultaneous determination of gaseous and particulate amines in practical environmental samples collected from industrial areas. Seven amines including MA, DMA, EA, DEA, DBA, CA, and TBA were found in gaseous and particulate phases in the industrial park. MA, DMA and DEA were the main amines in both particulate and gaseous samples. Comparison of the measured and predicted values showed that the gas-particle partitioning of amines in this study was mostly affected by acid-base reaction in particles, rather than physical absorption or simple gas-pure water conversion. Different from CA, which is more likely to enter the condensed phase by direct dissolution, DBA is more likely to enter the particle phase by reacting with acid gas.

Acknowledgments

This work was supported from the National Natural Science Foundation of China (Nos. 42020104001 and 41805103), Local Innovative and Research Team Project of Guangdong Pearl River Talents Program (No. 2017BT01Z032) and the Fund from Chemistry and Chemical Engineering Guangdong Laboratory (No. 1922009).

Appendix A Supplementary data

Supplementary material associated with this article can be found in the online version at doi:10.1016/j.jes.2021.09.027.

REFERENCES

Akyüz, M., 2007. Simultaneous determination of aliphatic and aromatic amines in indoor and outdoor air samples by gas chromatography–mass spectrometry. Talanta 71, 486–492.

Almeida, J., Schobesberger, S., Kürten, A., Ortega, I.K., Kupiainen-Määttä, O., Praplan, A.P., et al., 2013. Molecular understanding of sulphuric acid–amine particle nucleation in the atmosphere. Nature 502, 359–363.

An, T., Zhang, D., Li, G., Mai, B., Fu, J., 2011. On-site and off-site atmospheric PBDEs in an electronic dismantling workshop in south China: gas-particle partitioning and human exposure assessment. Environ. Pollut. 159, 3529–3535.

Bidleman, T.F., 1988. Atmospheric processes. Environ. Sci. Technol. 22, 361–367.

Carslaw, K.S., Clegg, S.L., Brimblecombe, P., 1995. A thermodynamic model of the system HCl-HNO_3-H_2SO_4-H_2O, including solubilities of HBr, from $<$200 to 328 K. J. Phys. Chem. 99, 11557–11574.

Chen, Y., Tian, M., Huang, R., Shi, G., Wang, H., Peng, C., et al., 2019. Characterization of urban amine-containing particles in southwestern China: seasonal variation, source, and processing. Atmos. Chem. Phys. 19, 3245–3255.

Cheng, G., Hu, Y., Sun, M., Chen, Y., Ge, X., 2019. Characteristics and potential source areas of aliphatic amines in $PM_{2.5}$ in Yangzhou, China. Atmos. Pollut. Res. 11, 296–302.

Chhibber-Goel, J., Gaur, A., Singhal, V., Parakh, N., Bhargava, B., Sharma, A., 2016. The complex metabolism of trimethylamine in humans: endogenous and exogenous sources. Expert Rev. Mol. Med. 18, e8.

De Haan, D.O., Hawkins, L.N., Kononenko, J.A., Turley, J.J., Corrigan, A.L., Tolbert, M.A., et al., 2011. Formation of nitrogen-containing oligomers by methylglyoxal and amines in simulated evaporating cloud droplets. Environ. Sci. Technol. 45, 984–991.

Fekete, A., Malik, A.K., Kumar, A., Schmitt-Kopplin, P., 2010. Amines in the Environment. Crit. Rev. Anal. Chem. 40, 102–121.

Ge, X., Shaw, S.L., Qi, Z., 2014. Toward understanding amines and their degradation products from postcombustion CO2 capture processes with aerosol mass spectrometry. Environ. Sci. Technol. 48, 5066–5075.

Ge, X., Wexler, A.S., Clegg, S.L., 2011a. Atmospheric amines – Part I. A review. Atmos. Environ. 45, 524–546.

Ge, X., Wexler, A.S., Clegg, S.L., 2011b. Atmospheric amines – Part II. Thermodynamic properties and gas/particle partitioning. Atmos. Environ. 45, 561–577.

Hanson, D.R., McMurry, P.H., Jiang, J., Tanner, D., Huey, L.G., 2011. Ambient pressure proton transfer mass spectrometry: detection of amines and ammonia. Environ. Sci. Technol. 45, 8881–8888.

Healy, R.M., Evans, G.J., Murphy, M., Sierau, B., Arndt, J., McGillicuddy, E., et al., 2015. Single-particle speciation of alkylamines in ambient aerosol at five European sites. Anal. Bioanal. Chem. 407, 5899–5909.

Ho, K.F., Ho, S.S.H., Huang, R., Chuang, H., Cao, J., Han, Y., et al., 2016. Chemical composition and bioreactivity of $PM_{2.5}$ during 2013 haze events in China. Atmos. Environ. 126, 162–170.

Huang, R.-J., Li, W.-B., Wang, Y.-R., Wang, Q.Y., Jia, W.T., Ho, K.-F., et al., 2014. Determination of alkylamines in atmospheric aerosol particles: a comparison of gas chromatography–mass spectrometry and ion chromatography approaches. Atmos. Meas. Tech. 7 (2014-07-04), 2027–2035.

Jastrzebska, A., Piasta, A., Szlyk, E., 2014. Simultaneous determination of selected biogenic amines in alcoholic beverage samples by isotachophoretic and chromatographic methods. Food Addit. Contam. Part A Chem. Anal. Control Expo Risk Assess. 31, 83–92.

Junninen, H., Ehn, M., Petäjä, T., Luosujärvi, L., Kotiaho, T., Kostiainen, R., et al., 2010. A high-resolution mass spectrometer to measure atmospheric ion composition. Atmos. Meas. Tech. 3, 1039–1053.

Kieloaho, A.-J., Hellén, H., Hakola, H., Manninen, H.E., Nieminen, T., Kulmala, M., et al., 2013. Gas-phase alkylamines in a boreal Scots pine forest air. Atmos. Environ. 80, 369–377.

Kürten, A., Jokinen, T., Simon, M., Sipilä, M., Sarnela, N., Junninen, H., et al., 2014. Neutral molecular cluster formation of sulfuric acid-dimethylamine observed in real time under atmospheric conditions. Proc. Natl. Acad. Sci. USA 111, 15019–15024.

Li, G., Liao, Y., Hu, J., Lu, L., Zhang, Y., Li, B., et al., 2019. Activation of NF-κB pathways mediating the inflammation and pulmonary diseases associated with atmospheric methylamine exposure. Environ. Pollut. 252, 1216–1224.

Liu, F., Bi, X., Zhang, G., Lian, X., Fu, Y., Yang, Y., et al., 2018. Gas-to-particle partitioning of atmospheric amines observed at a mountain site in southern China. Atmos. Environ. 195, 1–11.

Liu, F.-X., Bi, X., Ren, Z., Zhang, G., Wang, X., Peng, P., et al., 2017. Determination of amines associated with particles by gas chromatography-mass spectrometry. Chin. J. Anal. Chem. 45, 477–482.

Liu, X., Du, E., 2020. Atmospheric Reactive Nitrogen in China: Emission, Deposition and Environmental Impacts. Springer.

Lohmann, R., Lammel, G., 2004. Adsorptive and absorptive contributions to the gas-particle partitioning of polycyclic aromatic hydrocarbons: state of knowledge and recommended parametrization for modeling. Environ. Sci. Technol. 38, 3793–3803.

Murphy, S.M., Sorooshian, A., Kroll, J.H., Ng, N.L., Chhabra, P., Tong, C., et al., 2007. Secondary aerosol formation from atmospheric reactions of aliphatic amines. Atmos. Chem. Phys. 7, 2313–2337.

Nielsen, C.J., Herrmann, H., Weller, C., 2012. Atmospheric chemistry and environmental impact of the use of amines in carbon capture and storage (CCS). Cheminform 41, 6684–6704.

Pankow, J.F., 2015. Phase considerations in the gas/particle partitioning of organic amines in the atmosphere. Atmos. Environ. 122, 448–453.

Perrone, M.G., Zhou, J., Malandrino, M., Sangiorgi, G., Rizzi, C., Ferrero, L., et al., 2016. PM chemical composition and oxidative potential of the soluble fraction of particles at two sites in the urban area of Milan, Northern Italy. Atmos. Environ. 128, 104–113.

Qiu, C., Zhang, R., 2013. Multiphase chemistry of atmospheric amines. Phys. Chem. Chem. Phys. 15, 5738–5752.

Qiu, Z., Li, G., An, T., 2021. In vitro toxic synergistic effects of exogenous pollutants-trimethylamine and its metabolites on human respiratory tract cells. Sci. Total Environ. 783, 146915.

Rampfl, M., Mair, S., Mayer, F., Sedlbauer, K., Breuer, K., Niessner, R., 2008. Determination of primary, secondary, and tertiary amines in air by direct or diffusion sampling followed by determination with liquid chromatography and tandem mass spectrometry. Environ. Sci. Technol. 42, 5217–5222.

Shen, W., Ren, L., Zhao, Y., Zhou, L., Dai, L., Ge, X., et al., 2017. C1-C2 alkyl aminiums in urban aerosols: insights from ambient and fuel combustion emission measurements in the Yangtze River Delta region of China. Environ. Pollut. 230, 12–21.

Simon, M., Heinritzi, M., Herzog, S., Leiminger, M., Bianchi, F., Praplan, A., et al., 2016. Detection of dimethylamine in the low pptv range using nitrate chemical ionization atmospheric pressure interface time-of-flight (CI-APi-TOF) mass spectrometry. Atmos. Meas. Tech. 9, 2135–2145.

Smith, J.N., Barsanti, K.C., Friedli, H.R., Ehn, M., Kulmala, M., Collins, D.R., et al., 2010. Observations of aminium salts in

atmospheric nanoparticles and possible climatic implications. Proc Natl Acad USA 107, 6634–6639.
Tong, D., Chen, J., Qin, D., Ji, Y., Li, G., An, T., 2020. Mechanism of atmospheric organic amines reacted with ozone and implications for the formation of secondary organic aerosols. Sci. Total Environ. 737, 139830.
Varghese, A.M., Karanikolos, G.N., 2020. CO_2 capture adsorbents functionalized by amine – bearing polymers: a review. Int. J. Greenhouse Gas Control 96, 103005.
You, Y., Kanawade, V.P., de Gouw, J.A., Guenther, A.B., Madronich, S., Sierra-Hernández7, M.R., et al., 2014. Atmospheric amines and ammonia measured with a chemical ionization mass spectrometer (CIMS). Atmos. Chem. Phys. 14, 12181–12194.
Zhang, H., Ren, S., Yu, J., Yang, M., 2012. Occurrence of selected aliphatic amines in source water of major cities in China. J. Environ. Sci. 24, 1885–1890.
Zhang, W.N., Zhong, J., Shi, Q., Gao, L., Ji, Y., Li, G., et al., 2021. Mechanism for rapid conversion of amines to ammonium salts at the air-particle interface. J. Am. Chem. Soc. 143, 1171–1178.
Zhou, S.Q., LiC, H., Yang, T., Chen, Y., Deng, C., Gao, Y., et al., 2019. Characteristics and sources of aerosol aminiums over the eastern coast of China: insights from the integrated observations in a coastal city, adjacent island and surrounding marginal seas. Atmos. Chem. Phys. 19, 10447–10467.